Since January 2020 Elsevier has created a COVID-19 resource centre with free information in English and Mandarin on the novel coronavirus COVID-19. The COVID-19 resource centre is hosted on Elsevier Connect, the company's public news and information website.

Industrial Crops & Products 132 (2019) 468–475

Contents lists available at ScienceDirect

Industrial Crops & Products

journal homepage: www.elsevier.com/locate/indcrop

In vitro evaluation of anthraquinones from *Aloe vera* (*Aloe barbadensis* Miller) roots and several derivatives against strains of influenza virus

Rocío Borges-Argáez[a,*], Reyna Chan-Balan[a,b], Lisseth Cetina-Montejo[a,b], Guadalupe Ayora-Talavera[b], Pablo Sansores-Peraza[c], Jesús Gómez-Carballo[b], Mirbella Cáceres-Farfán[a]

[a] Unidad de Biotecnología, Centro de Investigación Científica de Yucatán, Calle 43 Número 130 × 32 y 34, CP 97205, Mérida, Yucatán, Mexico
[b] Departamento de Virología, Centro de Investigaciones Regionales "Dr. Hideyo Nogüchi", Calle 96 s/n ×, Av. Jacinto Canek y calle 47 Paseo de Las Fuentes, CP 97225, Mérida, Yucatán, Mexico
[c] Facultad de Química, Universidad Autónoma de Yucatán, Calle 43 Número 613 × calle 90, Colonia Inalambrica, CP 97069, Mérida, Yucatán, Mexico

ARTICLE INFO

Keywords:
Aloe vera
Anthraquinone
AH1N1
Influenza
Resistant strains
Aloesaponarin

ABSTRACT

Aloe vera is a crop of wide economic value of worldwide distribution, and a rich source of quinone components. Recently, antiviral aloe anthraquinones had been reported against human influenza virus.

In the present work two anthraquinones, aloesaponarin-I (**1**) and aloesaponarin-II (**2**) were isolated from *A. vera* roots, and six derivatives were obtained by methylation (**3**), acetylation (**4**) and *O*-glycosyl (**5-6**) reactions starting from (**1**). Additionally, a new Tetra-*O*-acetyl-β-D-glucopyranosyl derivative from **2** was also prepared. All compounds were evaluated against two strains of influenza virus AH1N1 by cytopathic effect reduction assay (CPE). The antiviral activity was determined by the ability of compounds to inhibit virus replication on Madin Darby Canine Kidney cells (MDCK). New derivatives 3-(2′,3′,4′,6′-Tetra-O-acetyl-β-D-glucopyranosyl-aloesaponarin-I (**5**) and *3*-(2′,3′,4′,6′-Tetra-O-acetyl-β-D-glucopyranosyl- aloesaponarin-II (**7**) showed a cytopathic reduction effect against influenza strain A/Yucatán/2370/09 with IC_{50} of 30.77 and 13.70 μM, and against the virus A/Mexico/InDRE797/10 with IC_{50} of 62.28 and 19.47 μM, respectively. To assess the effect of derivatives **5** and **7** during one cycle of replication (0–10 h), a time-of-addition experiment was performed. As a result it was found that both compounds were most effective when added 6–10 h post-infection and significantly inhibited viral titre (> 70%) at the concentrations of 50 and 100 μM. Based on the structural analysis of the compounds, it was suggested that the Tetra-O-acetyl-β-D-glucopyranosyl substituent at the C3 position of the anthraquinone might have an effect against the influenza AH1N1 virus.

1. Introduction

Aloe vera (Aloe barbadensis Miller) is the most widely used species, both commercially and for its therapeutic properties (Cardarelli et al., 2017; Kojo and Qian, 2004; Chen et al., 2012). This plant contains two materials with a juicy consistency: the first, a yellow exudate containing a high concentration of anthraquinone-type compounds, which have been used for decades as cathartics and purgatives, and the second, a clear mucilaginous gel that has been used since ancient times for the treatment of burns and other wounds (Fox et al., 2017; Reynolds and Dweck, 1999). Among the chemical components of the exudate are aloin, emodin, aloe-emodin, barbaloin, isobarbaloin and chrysophanic acid. These compounds have been shown to possess antibacterial, fungicidal, diuretic, laxative, antiviral, hepatoprotective and vasorelaxant activities (Salah et al., 2017; Drudi et al., 2018). The gel is highly rich in polysaccharides which are responsible of the immunostimulant and anti-inflammatory properties of the gel. Just over 200 different types of molecules have been isolated from this species, of which more than 75 different active compounds have been identified (Hamman, 2008; Reynolds, 1985). In southeast Mexico, the production of aloe leaves covers an area of approximately 222 ha (SIAP, 2015). Locally, the commercialization of aloe products is based on the concentrated gel from the leaves for the cosmetic industry. Some producers also commercialize the aloin obtained from the leave exudate for the pharmaceutical industry. In both processes, a high content of solid and agricultural residues is generated. The roots are not used locally as raw materials, but they are raising pharmaceutical interest because of their quinone content. Despite their many pharmacological activities and the

* Corresponding autor at: Centro de Investigación Científica de Yucatán, Calle 43 Número 130 × 32 y 34, CP 97205, Mérida, Yucatán, Mexico.
E-mail address: rborges@cicy.mx (R. Borges-Argáez).

https://doi.org/10.1016/j.indcrop.2019.02.056
Received 22 August 2018; Received in revised form 19 February 2019; Accepted 28 February 2019
Available online 07 March 2019
0926-6690/

available material, only aloe-emodin, emodin, and chrysophanic acid has been tested against influenza A virus (IAV) (Li et al., 2014).

IAV is a segmented, negative-sense, enveloped single-stranded RNA virus belonging to the family *Orthomyxoviridae* (Taubenberger, 2008; Bouvier and Palese, 2008). Infection with this virus cause respiratory disease in humans and animals with high morbidity and mortality rates (Iglesias et al., 2011; Naesens et al., 2016). Vaccination prevents influenza virus infection and antiviral drugs are used to treat infected patients; however, both are hampered by high variability of IAV surface glycoproteins (NA and HA mainly) and the emergence of resistant strains (Burnham et al., 2013; Li et al., 2015; McKimm-Breschkin, 2013). Considering the broad pharmacological activities of *A. vera* quinones, the aim of this study was to investigate the antiviral activity of aloesaponarin-I, aloesaponarin-II, and their derivatives against influenza A virus. This study is also a contribution to the knowledge of the potential pharmaceutical use of *A. vera* crops and industrial residues.

2. Materials and methods

2.1. Chemicals and reagents

Analytical TLC was carried out using aluminium-silica gel (60F254) plates (E.M. Merck, 0.2 mm thickness). Chromatographic purifications were performed using silica gel 60 (0.040–0.063 mm; Merck). The detection of the components under UV/Vis light at 254 and 365 nm was performed using a UV cabinet. The various components in the chromatograms were visualized using a solution of phosphomolybdic acid (20 g) and ceric sulfate (2.5 g) in 500 mL of sulfuric acid (5%), followed by heating. A specific reagent for quinone detection was used (Börntrager reagent). Gel permeation column chromatography was carried out using Sephadex LH-20 from Pharmacia. Chemical solvents and reagents for quinone derivatization, such as sodium hydroxide, dimethyl sulfate, potassium carbonate, anhydrous dichloromethane, tetrabutyl ammonium bromide and tetra-*o*-acetyl glucose bromide were commercially obtained from Fluka, Fermont or Sigma-Aldrich and were all analytically pure.

2.2. Plant material, extraction and purification of metabolites **1** and **2**

Roots of *A. vera* were collected on 22 May 2015 from a plantation belonging to Mr Abelino Pool in the municipality of Maxcanu, Yucatan, Mexico. The roots were air-dried and ground on a Brabender Dusiburg mill using a No. 2 sieve. Powdered roots (2.65 kg) were extracted three times with cold MeOH at room temperature for 72 h (1 L MeOH for each 500 g of dried material) (Fig. 1). The extracts were combined, and the solvent was removed under pressure to produce 326 g of crude methanolic extract. Then, 201 g of the extract were suspended in a 1:1 mixture of water/MeOH (*ca.* 150 mL of solution/ 20 g of crude methanolic extract), and the resulting suspension was partitioned with EtOAc to yield a medium polarity extract (37.37 g). Successive flash chromatography using a gradient elution with mixtures of *n*-hexane/AcOEt/MeOH and *n*-hexane/acetone of 2.23 g of AcOEt extract resulted in the isolation of metabolites **1** (112 mg) and **2** (20 mg) in pure form. Further purification of the AcOEt extract obtained additional amounts of compounds **1** (122.70 mg) and **2** (30.40 mg).

2.3. General experimental procedures for the derivatization of metabolites **1** and **2**

Metabolite **1**, which was obtained in good yield (5%), was subjected to chemical modification by methylation, acetylation and *O*-glycosyl reactions. Additionally, a tetra-*O*-acetyl-β-D-glucopyranosyl derivative from **2** and penta-acetyl glucose were also prepared. Briefly, for the methylation reaction, a mixture of **1** (50 mg, 0.16 mmol), CH_3I (1 ml) and K_2CO_3 (55 mg) in 10 mL of acetone was left to stir at room temperature for 72 h and then diluted with 30 mL of water. The resulting solution was extracted with ethyl acetate (3 × 30 mL). After the evaporation of the solvent, 43.22 mg (86.44% yield) of compound **3** were obtained as orange needles. For the acetylation reaction, a mixture of **1** (26.50 mg, 0.08 mmol), acetic anhydride (1 mL) and pyridine (0.50 mL) was allowed to stir overnight at room temperature. The reaction mixture was poured over water (50 mL), and the resulting suspension was extracted with ethyl acetate (3 times 1:1). The organic layer was washed (1:1, v:v) successively with water, 5% HCl, 5% $NaHCO_3$, and a NaCl saturated solution. The treatment of the solvent with anhydrous Na_2SO4 followed by filtration and evaporation yielded 21 mg (62.50% yield) of pure compound **4**. Finally, for the preparation of *O*-glucosyacetyl and *O*-glucosyl derivatives, we employed phase-transfer reactions following the general procedure reported by Halazy et al. (1990). Briefly, in a hermetically sealed container containing tetrabutylammonium bromide, a solution of the natural compound in anhydrous CH_2Cl_2 was added, and it was stirred for a minute. Then, a 5% v / v NaOH solution was added, and the mixture was allowed to stir for 3 min until a colour change occurred. Then, distilled water was added. Subsequently, a solution of acetobromo-α-D-glucose in anhydrous CH_2Cl_2 was added. The volume was adjusted with distilled water to a ratio of 1: 1 between the organic phase and the aqueous phase. The mixture remained under stirring at room temperature for 40 h. After the time period, the mixture was adjusted to pH 5 with a 5% v / v HCl solution. 50 mL of distilled water was added, and it was extracted with CH_2Cl_2 (3 × 40 mL), dried over anhydrous Na_2SO_4 and filtered. The solvent was evaporated to obtain *O*-glucosyacetyl derivatives. From 55.90 mg (0.17 mmol) of compound **1**, 102.30 mg of *O*-glucosyacetyl compound **5** (88.95% yield) was obtained. Additionally, 25.60 mg (0.10 mmol) of compound **2** gave 27 mg of compound **7** (45.91%). To obtain *O*-glucosyl derivative **6**, 26 mg (0.04 mmol) of compound **5** was

Fig. 1. Collection of *Aloe vera* roots and methanolic extraction.

dissolved in 22 mL of ethanol, and 1 mL of HCl was added. The mixture was stirred and warmed up to 70 °C for 2 h under reflux. Once cooled, the solution was dried on a rotary evaporator. The residue was purified by flash column chromatography employing 100% EtOAc to yield 5.80 mg (30.21% yield) of derivative **6** as a yellow powder. NMR was employed for the chemical characterization of compounds **1**-**7**.

2.4. Spectroscopic characterization

For the chemical characterization, ^{1}H NMR (400 MHz) and ^{13}C NMR (100 MHz) spectra were obtained on a Bruker Avance 400 spectrometer using the residual $CHCl_3$ signal (7.26 and 77.00 ppm for ^{1}H and ^{13}C respectively) and MeOH residual signals (3.35 and 4.78 for ^{1}H and 49.30 for ^{13}C) as references. Gas chromatography and mass spectrometry (CG-EM) analyses were run on an Agilent Technologies Chromatographer model 6890 N coupled to a mass spectrometer, model 5975B, using the following chromatographic conditions: split injection of 1 µL of a 1% concentration sample; Ultra 1 column (25 m × 0.32 D, 0.52 µm layer thickness), flow rate 1.5 mL/min (helium as carrier gas); oven temperature programme T150 ± SD (µM) = 120 °C (2 min), Ta = 325 °C (20 min), gradient 10 °C/min, injector and detector temperature (FID) at 280 °C. The LC-HRMS data were acquired on a Bruker mXis-QTOF mass spectrometer (Bruker Daltonics GmbH, Bremen, Germany) coupled to the LC system. The mass spectra were collected from 150 *m/z* to 2000 *m/z* in positive mode

2.5. Cells and viruses

Viral tests, the Madin Darby Canine Kidney cell line (Madin-Darby Canine Kidney) cells, and the Influenza viruses A/Yucatán/2370/09 (susceptible to oseltamivir) and A/Mexico/InDRE797/10 (resistant to oseltamivir) were provided by the Virology Laboratory of the Regional Research Centre at the Universidad Autonoma de Yucatán, México.

2.6. Cytotoxicity

MDCK cells were grown in a 96-well plate at a cell density of 1 × 10^{5} cells per well and incubated at 37 °C with 5% CO_2 for 24 h. The cells were washed twice with PBS (pH 7.20, GIBCO). Soon after, the cells were incubated with 100 µL of compounds (dilutions were in a range of 100 to 3.12 µM in D-MEM for 72 h at 37 °C and 5% CO_2. After incubation, the cells were fixed and stained with 0.40% crystal violet in methanol. The absorbance was measured at a wavelength of 490 nm in a Multilabel Plate Reader (Victor 3 x Perkin-Elmer 2030). The assay was performed in triplicate. Cell viability was determined from the ratio between the optical density (OD) of the treated cells and the OD of the cell control, considering 100% viable cells:

% Cell viability = (OD treated cells / OD cell control) × 100).

The 50% cytotoxic concentration was calculated by regression analysis.

2.7. Antiviral assays

2.7.1. Cytopathic effect (CPE) reduction assay

MDCK cells were seeded at a cell density of 5 × 10^{4} cells / well and incubated for 24 h at 37 °C in 5% CO_2. To measure the CPE reduction effect, the cells were infected with the influenza virus at a MOI of 0.01 in the presence of various concentrations of the compounds (100 to 3.12 µM) in1X Dubelco´s Modified Eagles Media D- MEM, GIBCO supplemented with TPCK trypsin (1 µg / mL) and incubated at 37 °C in 5% CO_2 for 72 h. After this time, CPE reduction was observed under a light microscope, and then, the cells were stained with 0.40% crystal violet in methanol. The OD was measured at a wavelength of 490 nm. CPE reduction was calculated using the formula:

$$\% \text{ CPE reduction} = [(A \times B) / (C \times B)] \times 100$$

where A is the OD of the cells infected and treated with the compounds, B is the OD of the virus control and C is the OD of cell control. The mean inhibitory concentration (IC_{50}) was defined as the concentration that inhibits the CEP reduction by 50% of the infected cells and was calculated by non-linear regression analysis using the GraphPad Prism programme, version 6.01.

2.7.2. Plaque reduction test

MDCK cells were seeded at a cell density of 5 × 10^{5} cells / well in 12-well plates for 24 h at 37 °C in 5% CO_2. The cell monolayers were incubated with serial dilutions (1 × 10^{-1} to 1 × 10^{-6}) of the supernatants of each concentration of compound in the CPE assay for 1 h. After this time, the inoculum was removed, and 3% agarose was added to the overlay medium, which was incubated for 72 h at 37 °C in 5% CO_2. Soon after, the agar was removed and stained with 0.40% crystal violet in methanol. The number of plates was counted, and the activity of the compounds was compared to the viral control and Oseltamivir control.

2.7.3. Time-of-addition experiments

To assess the effects of derivatives **5** and **7** during a viral cycle (0–10 h), a time-of-addition experiment was performed as previously described (Zhang et al., 2012; Yamada et al., 2012; Furuta et al., 2005) (Fig. 2). Briefly, cells were seeded into 24-well plates and incubated with influenza virus A/Yucatán/2370/09 (A/Yuc/2370/09) and the strain A/Mexico/InDRE797/10 (A/InDRE/10) (MOI of 1). After one hour of viral absorption, the monolayers were incubated with DMEM and 0.50 µg / mL of trypsin-TPCK in 5% CO_2 at 37 °C (time zero). The medium containing the compounds (50 µM) was added at times 0–2, 2–4, 4–6, 6–8, 8–10 and 0–10 h. After each incubation, the inoculum was removed. Then, fresh medium was added and incubated until 10 h post-infection. The supernatants were collected, and viral production was determined by plaque assays.

2.8. Statistic analysis

The results are represented as the average of three independent experiments ± the standard deviation. A one- and two-way ANOVA analysis was performed to determine if there are significant differences

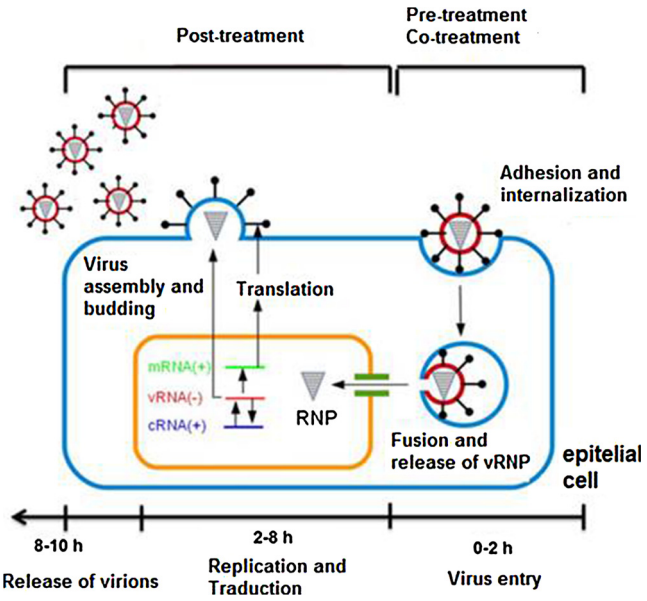

Fig. 2. General outline of the stages of the influenza virus cycle and its evaluation by Time-of-addition experiments.

with respect to the controls.

3. Results

3.1. Extraction and isolation of metabolites 1 and 2

From the AcOEt extract of roots of *A. vera,* metabolites **1** and **2** were obtained in pure form with a yield of 5 and 1.35%, respectively. Both metabolites showed the following physical characteristics:

Aloesaponarin I (**1**): oranges crystals, soluble in $CHCl_3$; ^1H NMR ($CDCl_3$, 400 MHz) δ), 2.96 (3H, s, H-11), 4.06 (3H, s, H-13), 7.30 (1H, dd, J = 8.3, 1.0 Hz, H-7), 7.62 (1H, t, J= 7.9 Hz, H-6), 7.76 (1H, dd, J= 7.4, 1.1 Hz, H-5), 7.78 (1H, s, H-4), 10.42 (1H, s, H-3), 12.92 (1H, s, H-8) (Yagi. et al.,1974).

Aloesaponarin II (**2**): oranges crystals, soluble in acetone. ^1H NMR ($[CD_3]_2CO$, 400 MHz) δ 2.66 (1H, s, H-11), 6.99 (1H, d, J= 2.3 Hz, H-2), 7.17 (1H, dd, J= 7.6, 2.1 Hz, H-5), 7.47 (1H, d, J= 2.3 Hz, H-4), (2H, m, H-6, H-7), 12.92 (1H, s, H-8) (Yagi et al.,1974).

3.2. Structure identification of derivatives 3–7

All derivatives were characterized using ^1H NMR and LC-HRMS together with GC/MS. Compounds **3**-**4** were readily deduced through a comparison of their spectroscopic data (^1H NMR, ^{13} C NMR) with the spectroscopic data found in the literature (Lee et al., 2007; Yagui et al., 1974), except for derivatives **5–7,** which were new structures. Compound **5** and **7** were all obtained as intermediate compounds from the *O*-glucosyl reaction of **1** and **2**. The ^1H NMR and ^{13}C NMR data, along with the molecular formula of compound **5**, indicated a tetracyclic skeleton containing two aromatic rings corresponding to a anthraquinone-type compound. The ^1H NMR spectrum of **5** also showed the expected four sugar acetyl signals at δ 2.04, 2.07, 2.10 and 2.18. The LC-HRMS spectra showed a single peak at a retention time of 7.75 min and a molecular ion peak at *m/z* value 642 (calcd for $C_{31}H_{30}O_{15}$). The ^2D NMR spectra allowed the complete characterization of derivative **5**. Using all the previously mentioned data, compound **5** was elucidated to be 3-(2´,3´,4´,6´-tetra-O-acetyl-β-D-glucopyranosyl)-Aloesaponarin I, a new derivative of **1**. Compound **7** was isolated as yellow needles and showed similar ^1H NMR and ^{13}C NMR data as **5**, except for the additional aromatic proton at δ7.14 (1H, d, J = 2.7 Hz) from the Aloesaponarin II anthraquinone structure. Consequently, compound **7** was determined to be new 3-(2´,3´,4´,6´-tetra-O-acetyl-β-D-glucopyranosyl)-aloesaponarin II. Derivative **6** was obtained as a yellow powder. The LC-HRMS spectra showed a single peak at a retention time of 3.50 min and a molecular ion peak at *m/z* value 474 (calcd for $C_{23}H_{22}O_{11}$). The IR spectrum had absorption bands at 3600 cm^{-1} (for hydroxyl groups), 1660 cm^{-1} (for conjugated carbonyl group), 1580 cm^{-1} (for aromatic rings) and 1730 cm^{-1} (for ester group). The ^{1}HNMR and ^{13}C NMR (CD_3OD) spectra of **6** indicated the presence of an anthraquinone structure [δ 7.31 (1H, dd, J = 1.2, 8.3 Hz, H-7); 7.69 (1H, t, J = 7.9 Hz, H-6); 7.74 (1H, dd, J = 1.2, 7.5 Hz, H-5); 7.97 (1H, s, H-4), having a β-D-glucopyranosyl anomeric proton at δ 5.25 (1H, d, J = 7.5 Hz, H-1´) in addition of an acetyl group (δ 3.97 (3H, s, acetyl CH3-13) and one methyl proton (δ 2.72 (3H, s, H-1). Furthermore, in the heteronuclear multiple bond connectivity (HMBC) experiment, long-range correlations were observed between the 1´-H proton and C3 carbon, confirming the sugar moiety on the aglycone. On the basis of this evidence, it was confirmed derivative **6** as a new aloesaponarin I derivative with a 3-O-β-D- glucopyranoside.

Derivatives **3**-**7** showed the following physical characteristics:

3,8-dimethoxy-aloesaponarin I (***3***): orange crystals, soluble in chloroform. ^1H NMR ($CDCl_3$, 400 MHz) δ 2.69 (3H, s, H-11), 3.97 (3H, s, H-14), 3.99 (3H, s, H-15), 4.03 (3H, s, H-13), 7.34 (1H, dd, J= 8.4, 0.9 Hz, H-7), 7.65 (1H, s, H-4), 7.67 (1H, *t*, J = 8.1 Hz, H-6), 7.87 (1H, dd, J = 7.7, 1.1, H-5) (Lee et al., 2007).

3,8-diacetoxy-aloesaponarin I (***4***): yellow crystals, soluble in chloroform. ^1H NMR ($CDCl_3$, 400 MHz) δ 2.32 (3H, s, 3-OAc), 2.47 (3H, s, 3-OAc), 2.68 (3H, s, H-11), 3.96 (3H, s, H-13), 7.42 (1H, dd, J= 8.1, 1.3 Hz, H-7), 7.75 (1H, t, H-6), 7.98 (1H, s, H-4), 8.18 (1H, dd, J = 7.7, 1.4, H-5) (Yagui et al., 1974).

3-(2´,3´,4´,6´-Tetra-O-acetyl-β-D-glucopyranosyl- aloesaponarin I (***5***) Dark yellow powder; m.p: 220–222 °C; LC-HRMS *m/z* [M + 1$^+$], $C_{31}H_{30}O_{15}$ = 642; UV $\lambda_{máx}^{CHCl_3}$: 245 nm. IR (KBr): 3030, 2956, 1642, 1738, 1674, 1642, 1579 cm^{-1}. ^1H NMR ($CDCl_3$ 400 MHz): δ 2.04(3H, s, H-4´´´), 2.07(3H, s, H-2´´´), 2.10 (3H, s, H-3´´´), 2.18 (3H, s, H-6´´´),2.74 (3H, s, H-11), 3.95 (3H, s, H-13), 4.11(1H, m, H-5´),4.28 (2H, dd, J = 3.8,0.2 Hz, H-6´), 5.35 (1H, m, H-2´), 5.15 (2H, dd, J = 9.3,10.1 Hz, H-4´), 5.24 (1H, d, J = 7.6, Hz, H-1´), 5.35 (2H, m, H-2´,3´), 7.32 (1H, dd, J = 8.4,1.2 Hz, H-7), 7.63 (1H, t, J = 8.0 Hz, H-6), 7.75 (1H, dd, J = 7.6, 1.2 Hz, H-5), 7.89 (1H, s, H-4), 12.76 (1H, s, H-8). ^{13}C NMR: δ 20.01 (C-11), 20.48 (C-6´´´), 20.52 (C-4´´´), 20.54 C-3´´´), 20.56 (C-2´´´), 52.96 (C-13), 61.92 (C-6´), 68.13 (C-4´),70.15 (C-2´), 72.18 (C-3´), 72.65 (C-5´), 98.57(C-1´), 110.83 (C-4), 116.82 (C-8a), 119.0(C-5), 125.05 (C-7), 126.44 (C-8b), 132.28 (C-2), 132.40 (C-4b), 136.05 (C-6), 137.34 (C-4a), 141.66 (C-1), 156.67 (C-3), 162.50 (C-8), 166.67 (C-12), 169.31 (C-2´´), 169.42 (C-3´´), 169.99 (C-4´´), 170.87 (C-6´´), 181.69 (C-10), 189.59 (C-9).

The ^1H NMR spectrum ($CDCl_3$, 400 MHz) of derivative **5** is shown in Fig. 3.

3-glucosil aloesaponarin I (**6**): Yellow powder; m.p: 183–185 °C; LC-HRMS *m/z* [M + 1$^+$], $C_{23}H_{22}O_{11}$ = 474; UV $\lambda_{máx}^{CHCl_3}$: 230, 275 nm. IR (KBr): 3440, 2920, 1730, 1715, 1660, 1630, 1580, 1460, 1280 cm^1. ^1H NMR (CD_3OD 400 MHz): δ 2.72 (3H, s, H-11), 3.45 (1H, dd, J = 4.8, 0.2 Hz, H-2´), 3.47 (1H, dd, J = 5.5, 0.2 Hz, H-4´), 3.49 (1H, dd, J = 7.5, 0.2 Hz, H-3´),3.58 (1H, m, H-5´),3.76 (1H, dd, J = 12.1, 5.0 Hz, H-6´), 3.97 (3H, s, H-13),7.31 (1H, dd, J = 8.3,1.2 Hz, H-7), 7.69 (1H, t, J = 7.9 Hz, H-6), 7.74 (1H, dd, J = 7.5, 1.2 Hz, H-5), 7.97 (1H, s, H-4), 12.91 (1H, s, H-8).^{13}C NMR: δ 20.30 (C-11), 53.33 (C-13), 62.24(C-6´), 70.91 (C-2´), 74.71 (C-4´), 78.10(C-3´), 78.52 (C-5´), 101.68(C-1´), 112.56 (C-4), 118.19 (C-8a), 119.88(C-5), 125.71 (C-7), 126.96 (C-8b), 133.31 (C-2), 134.08 (C-4b), 137.27 (C-6), 138.68 (C-4a), 142.47 (C-1), 158.90 (C-3), 163.57(C-8), 168.82 (C12), 183.20(C-10), 191.15 (C-9).

3-(2´,3´,4´,6´-Tetra-O-acetyl-β-D-glucopyranosyl- aloesaponarin II (***7***): Dark yellow powder; LC-HRMS [M + 1$^+$], $C_{29}H_{28}O_{13}$ = 584; UV $\lambda_{máx}^{CHCl_3}$: 266 nm. IR (KBr): 2919, 1744, 1619, 1593, 1459 cm^{-1}. ^1H NMR ($CDCl_3$ 400 MHz): δ 2.05(3H, s, CH3–4´´´), 2.07(6H, s, H-3´´´, H-4´´´), 2.11(3H, s, H-2´´),2.83 (3H, s, H-11), 4.03 (1H, m, H-5´), 4.24 (1H, m, H-6´), 5.17 (1H, m,H-4´), 5.34 (3H, m, H-1´, H-2´, H-3´), 7.14 (1H, d, J = 2.7 Hz, H-2),7.30 (1H, dd, J = 8.4,1.2 Hz, H-5), 7.62 (1H, t, J = 7.9 Hz, H-6), 7.76 (1H, d, J = 2.9 Hz, H-4), 7.77 (1H, dd, J = 7.5,1.3 Hz, H-7),12.91 (1H, s, H-8). ^{13}C NMR: δ 20.52 (C-4´´´), 20.55(C-3´´´, C-6´´´), 20.57 (C-2´´´), 23.97 (C-11), 61.94 (C-6´), 68.14 (C-4´),70.96 (C-3´), 72.56 (C-5´), 75.45 (C-2´), 97.59(C-1´), 111.84 (C-7),116.83 (C-8a),118.89(C-4), 124.76 (C-5), 126.21 (C-2), 126.28 (C-8b), 132.81 (C-4b), 135.83 (C-6), 137.38 (C-4a),145.61 (C-1), 159.85 (C-3), 162.49 (C-8), 167.70 (C-2´´), 169.38 (C-3´´), 170.06 (C-4´´),170.66 (C-6´´), 182.39 (C-10), 189.94(C-9).

All spectroscopic data of new derivatives **5**-**7** are available online as supplementary material.

3.3. Cytotoxicity and CPE effect results

The cytotoxicity and cytopathic reduction (CPE) effects of natural anthraquinone **1** and **2** and derivatives **3**-**7** (Fig. 4) together with a penta-acetyl sugar, were evaluated. None of the quinones and penta-acetyl sugar showed a significant cytotoxic effects (CC_{50} > 90 μM) in MDCK cells, indicating 100% cell viability at all the concentrations tested. We then assessed CPE reduction, as observed in Table 1, compound **2** showed weak CPE reduction (IC_{50} = 62.31 μM) with the susceptible strain, with IC_{50} values similar to those presented by compound **5** with the resistant strain. In contrast, compound **7**

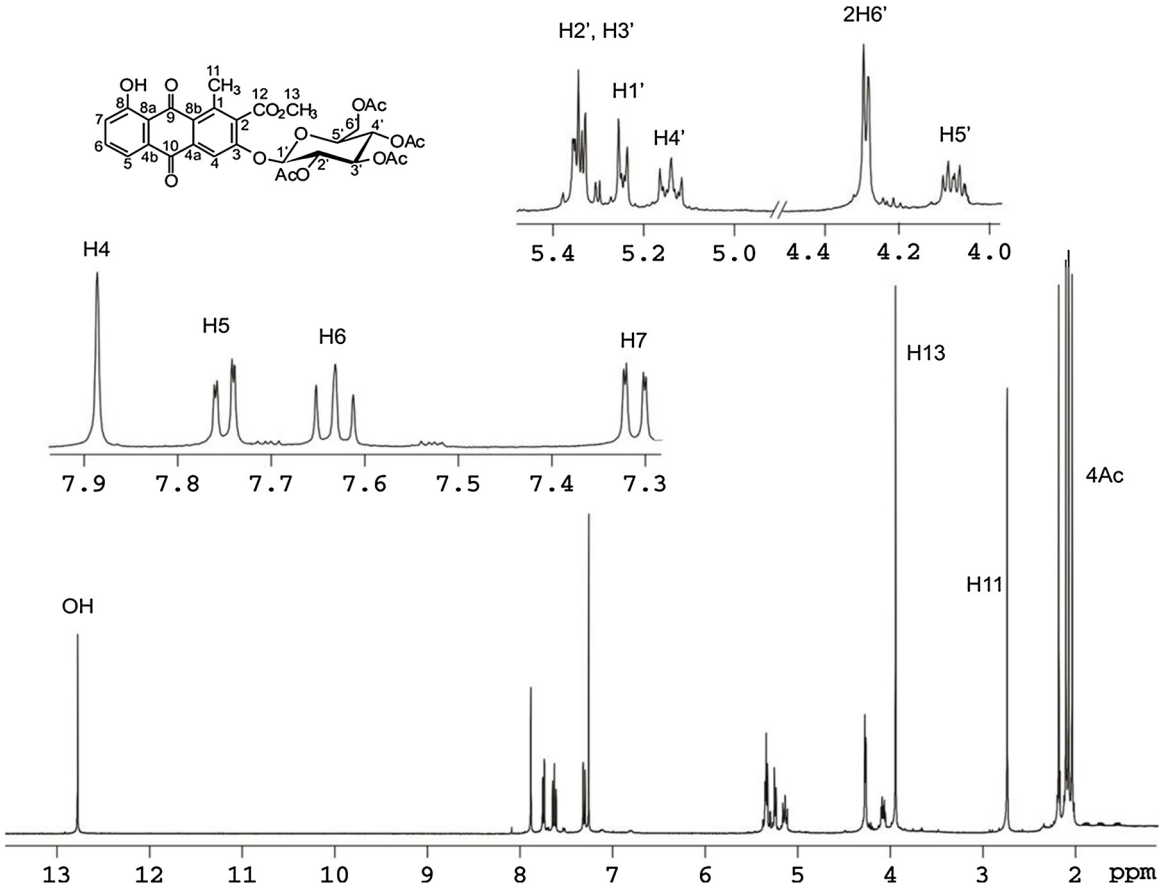

Fig. 3. The ^{1}H NMR spectrum ($CDCl_3$, 400 MHz) of derivative **5**.

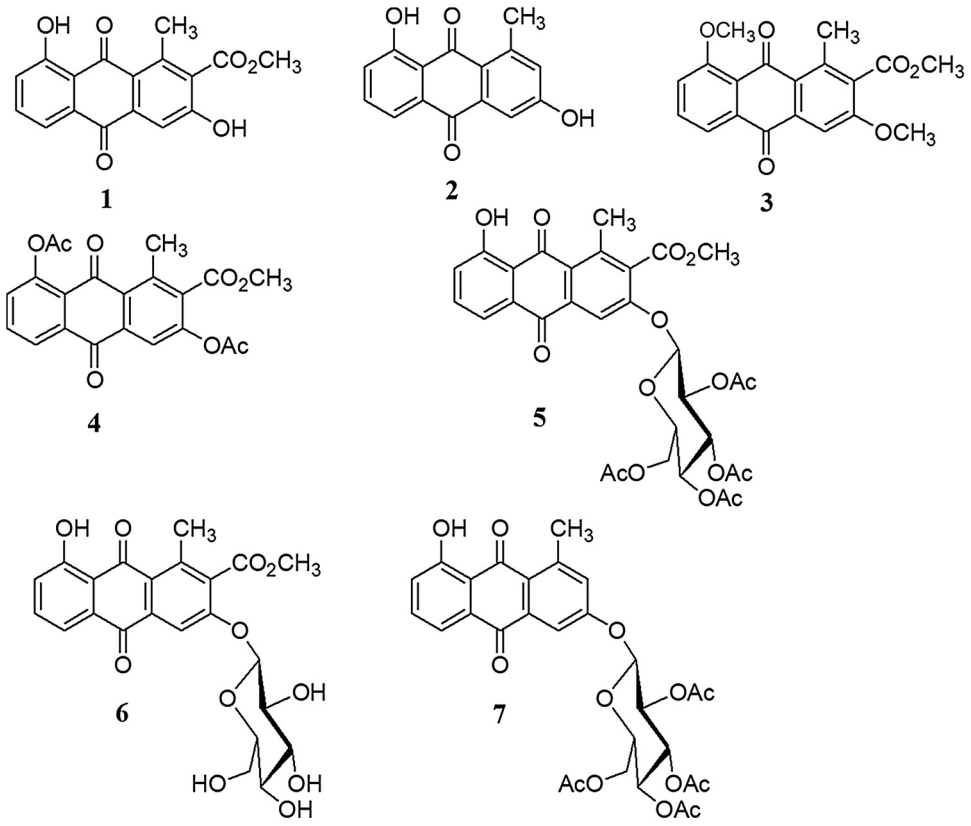

Fig. 4. Aloesaponarin I (**1**) and II (**2**) and derivatives **3**-**7**.

Table 1
The cytotoxic and antiviral activity of compounds **2**, **5** and **7**.

Compound	CC_{50}	IC_{50} (μM ± SD)[a] A/Yucatán/2370/09	IC_{50} (μM ± SD)[a] A/México/InDRE797/10
2	> 100	62.31 ± 3.05	NA
5	> 100	30.77 ± 2.10	62.28 ± 2.65
7	> 100	13.70 ± 3.80	19.47 ± 0.93
OC	> 100	0.025 ± 0.05	R

CC_{50}: Half maximal cytotoxic concentration.
IC_{50}: Inhibitory concentration.
NA: No activity.
OC: Oseltamivir carboxylate as a positive control.
R: resistant virus to OC.
[a] Mean values of three replicates.

(IC_{50} = 13.70 μM) was twice as effective with the susceptible strain in comparison of compound **5**. The derivatives **1, 3**-**4** and **6** and the penta acetyl sugar did not have antiviral activity. These results suggest that the presence of a tetra-*O*-acetyl-β-D-glucopyranosyl substituent at the C3 position of the anthraquinone might have an effect against influenza AH1N1 viruses.

3.4. Plaque inhibition test

Next, to assess if the results of the CPE using compounds **5** and **7** correlated with a reduction in viral yield, post-treatment experiments were done using a plaque inhibition assay to determine viral titres at serial dilution concentrations. Each compound was evaluated in triplicate using the A/Yuc/2370/09 strain. In this experiment, infectious particles were titrated from the viral samples obtained directly from the post-treatment. As shown in Fig. 5, the behaviour of compound **5** was dose-dependent, which significantly reduced the viral titre at the concentrations of 100 and 50 μM. However, the antiviral activity drastically decreased at the lowest concentrations evaluated. On the other hand, compound **7** also had dose-dependent behaviour. The antiviral activity was maintained in a range between 40–60% and was found to be less active than compound **5**.

3.4.1. Time-of-addition experiments

The effect of compounds **5** and **7** on a single-cycle of replication (0–10 h) in influenza virus was performed using 50 μM of the compounds. The life cycle of the influenza virus lasts from 8 to 10 h and can be divided into three stages: a) viral entry (0–2 h), b) replication and translation of the viral genome (2–8 h) and c) release of the viral progeny (8–10 h). Each stage is a pharmacological target of inhibitory molecules. In this way, compounds **5** and **7** were added at 5 different times during viral infection. Based on the IC_{50} values (IC_{50} < 25 μM), both compounds were evaluated using the A/Yuc/2370/09 virus. As seen in Fig. 6, both compounds decreased the viral production by 70% when added at 6–10 h post-infection. In the same manner, compound **7** reduced viral production of the A/InDRE/10 virus by 60% at the same period of time, 6–10 h. These results suggest that both compounds **5** and **7** inhibit viral production during virus infection.

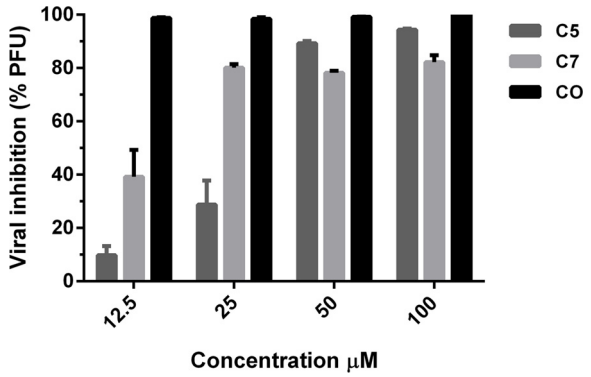

Fig. 5. A plaque reduction assay of compounds **5** and **7** against Influenza A/Yuc/2370/09 (0.01 MOI).

4. Discussion

This work describes the isolation, derivatization and antiviral evaluation of the main anthraquinones obtained from the roots of *A. vera*. ^{1}H NMR, ^{13}C NMR, 2D experiments and LC-HRMS of compounds **5**-**7** allowed for the complete characterization of new 3-2′,3′,4′,6′-tetra-O-acetyl-β-D-glucopyranosyl- 910 anthraquinone derivatives, where derivative **5** was obtained in good yield (88%). For the antiviral evaluation, several *in vitro* assays were performed based on indirect (CPE reduction assay) and direct (Plaque inhibition test, Time-of-addition experiments) methods. On the former, the ability of compounds to inhibit virus replication on MDCK cells was measured. On the latter, the ability of compounds to reduce viral titers was determined (Sidwell and Smee, 2000; Chattopadhyay et al., 2009). The plaque reduction assay and time-of-addition results suggested that the antiviral activity of compounds **5** and **7** increases at the post-treatment level.

The structure-activity relationship between the influenza virus and isolates **1** and **2** together with their derivatives (**3** to **7**) was assessed. As a result we found that acetylation, methylation and O-glycosyl addition does not improve the antiviral activities of compounds **1** and **2**; however if an acetyl sugar is added a moderate antiviral effect is observed. Besides, the acetylated glucose by itself was unable to cause a CPE reduction against influenza viruses.

Based on the analysis of the structure-activity relationship it is inferred that: 1) the tetraacetylated glucose residue at position 3 in compound **5** and **7** has an important role on the antiviral activity; 2) the tetraaceylated glucose by itself has no anti-influenza effect and therefore the binding of O-glucosyl to the anthraquinone is relevant for antiviral activity; 3) the lipophilicity also plays an important role since the polar derivative **6** (with glucose at position 3) was not active in contrast to the O-tetraacetylglucosylated compound.

A probable explanation of the antiviral activity of **5** and **7** may be due to the structural similarity between the tetraacetylated glucose residue and the sialic acid receptor, both with an oxygenated cyclohexane structural core, increasing the interaction either with the virus hemagglutinin (HA) and/or the viral sialidase (neuraminidase) (Nishikawa et al., 2012). On the contrary, none of the aglycones showed antiviral activity except aglycone 2, which lacks the acetyl group at position 2.

According to the literature, only a few studies describing the antiviral structure-activity relationship of quinones has been reported. *In silico* studies on juglone, made by Yang et al. (2013) pointed out that this quinone is able to interact with HA and NA glycoproteins of influenza virus, and this interaction is mainly with the 2-ciclohexenone-1,4-dione ring, and for the formation of strong hydrogen bridges with the active site. In another study, Bodian et al. (1993) mentioned that quinones are fusion inhibitory molecules of influenza virus, and their share structure similarities as the presence of an hidrofobic ring between 2 and 3 position, and an hidrofobic sustituent at C-2 as in compound **5** and **7**.

The antiviral activity of natural quinones and some derivatives isolated from plants has been demonstrated for parainfluenza virus (Andersen et al., 1991); SARS-CoV (Park et al., 2012) and influenza A virus (Li et al., 2014; Sydiskis et al., 1991; Feng et al., 2015; Wang et al., 2016). However, no information about the influence of the addition of an O-tetraacetylglucosylated group on aloe anthraquinones **1** and **2**, and its effect on inhibition on influenza A virus.

The presented results encourage further studies on anthraquinone derivatives, especially those with an O-tetraacetylglucosylated group, and further *in vitro* and *in vivo* experiments due to the high abundance

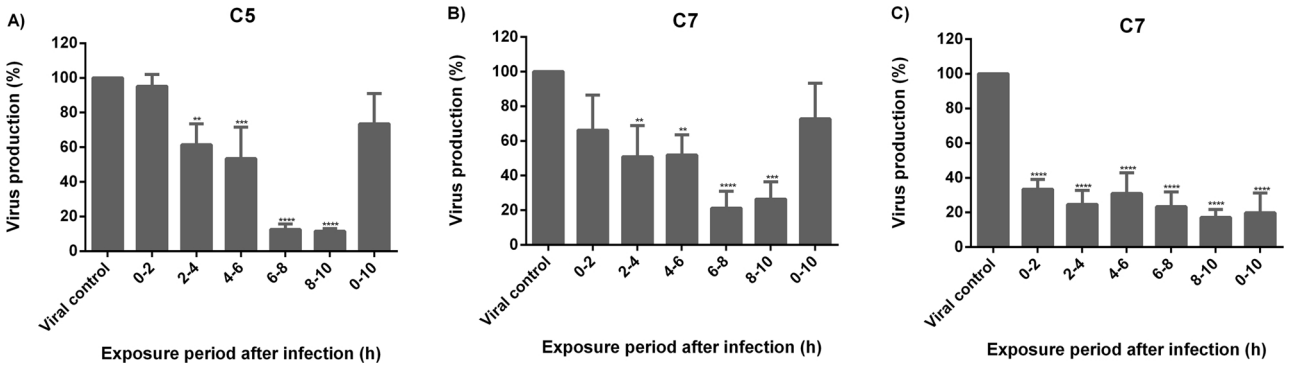

Fig. 6. The effect of anthraquinones **5** and **7** on a single-cycle replication of Influenza virus using 50 μM of each compound. MDCK cells were infected with: A) and B) A/Yuc/2370/09 (MOI of 0.1) and C) A/ InDRE797/10 (MOI of 1). Viral titres were determined at different hours using the plaque assay. Data are expressed as the mean ± SD of three independent replicates. **P < 0.01, ***P < 0.001, ****P < 0.0001.

of this material in *A. vera* crops and agroindustrial residues.

5. Conclusions

In this study, we report for the first time the characterization and chemical modification of the main anthraquinones of *A. vera* roots. In an attempt to demonstrate a new potential use of anthraquinones and their derivatives, our results suggest possible antiviral activity against influenza A virus and two new derivatives 3-*O*-tetraacetoglupiranosyl of aloesaponarin I and aloesaponarin II. These results add value to *A. vera* crop, and could be considered a promising source of either raw material or new derivatives for potential pharmaceutical interests.

Conflict of interests

The authors declare no conflicts of interest.

Acknowledgements

This work was financially supported by CONACYT (Project number SSA-2010-126763 and FOMIX-Gobierno del Estado de Yucatán project number 170130). We are grateful to CONACYT for supporting Chan-Balan and CetinaMontejo in their grants for the master degree at CICY.

Appendix A. Supplementary data

Supplementary material related to this article can be found, in the online version, at doi:https://doi.org/10.1016/j.indcrop.2019.02.056.

References

Andersen, D.O., Weber, N.D., Wood, S.G., Bronwyn, H.G., North, J.A., 1991. *In vitro* virucidal activity of selected anthraquinones and anthraquinone derivatives. Antiviral Res. 16, 185–196. https://doi.org/10.1016/0166-3542(91)90024-L.

Bodian, D.L., Yamasaki, B.R., Buswell, R.L., Stearns, J.F., White, J.M., Kuntz, I.D., 1993. Inhibition of the fusion-inducing conformational change of influenza hemagglutinin by benzoquinones and hydroquinones. Biochemistry 32, 2967–2978.

Bouvier, N.M., Palese, P., 2008. The biology of influenza virus. Vaccine 12, 49–53. https://doi.org/10.1016/j.vaccine.2008.07.039.

Burnham, A.J., Baranovich, T., Govorkova, E.A., 2013. Neuraminidase inhibitors for influenza B virus infection: efficacy and resistance. Antiviral Res. 100, 520–534. https://doi.org/10.1016/j.antiviral.2013.08.023.

Cardarelli, M., Rouphael, Y., Pellizzoni, M., Colla, G., Lucini, L., 2017. Profile of bioactive secondary metabolites and antioxidant capacity of leaf exudates from eighteen *Aloe* species. Ind. Crops Prod. 108, 44–51. https://doi.org/10.1016/j.indcrop.2017.06.017.

Chattopadhyay, D., Chawla- Sarkar, M., Chatterjee, T., Dey, R.S., Bag, P., Chakraborti, S., Khan, M.T.H., 2009. Recent advancements for the evaluation of anti-viral activities of natural products. New Bioeth. 5, 1–22. https://doi.org/1016/j.nbt.2009.03.007.

Chen, W., Van Wyk, B.E., Vermaak, I., Viljoen, A.M., 2012. Cape aloes-a review of the phytochemistry, pharmacology and commercialisation of Aloe ferox. Phytochem. Lett. 5, 1–12. https://doi.org/1016/j.phytol.2011.09.001.

Drudi, D., Tinto, D., Ferranti, D., Fiorelli, F., Dal Pozzo, M., Capitani, O., 2018. *Aloe barbadensis* miller versus silver sulfadiazine creams for wound healing by secondary intention in dogs and cats: a randomized controlled study. Res. Vet. Sci. 117, 1–9. https://doi.org/1016/j.rvsc.2017.10.010.

Feng, Z., Shuai, Z., Jing-Tian, H., Yuan-Fang, W., Ya-Nan, W., Chun-Hua, W., 2015. Antiviral anthraquinones from the roots of *Knoxia valerianoides*. Phytochem. Lett. 11, 57–60. https://doi.org/1016/j.phytol.2014.11.015.

Fox, L.T., Mazumber, A., Dwivedi, A., Gerber, M., Hamman, J.H., 2017. *In vitro* wound healing and cytotoxic activity of the gel and whole-leaf materials from selected aloe species. J. Ethnopharmacol. 200, 1–7. https://doi.org/1016/j.jep.2017.02.017.

Furuta, Y., Takahashi, K., Sangawa, H., Kuno-Maekawa, M., Uehara, S., Nomura, N., Kozaki, K., Egawa, H., Shiraki, K., 2005. Mechanism of action of T-705 against influenza virus. Antimicrob. Agents Chemother. 49, 981–986. https://doi.org/10.1128/AAC.49.3.981-986.2005.

Halazy, S., Berges, V., Ehrhard, A., Danzin, C., 1990. *Ortho*-and *para*-(diflouromethyl) aryl-β-glucosides: a new class of enzyme-activated irreversible inhibitors of β-glucosidases. Bioorg. Chem. 18, 330–344. https://doi.org/10.1016/0045-2068(90)90007-R.

Hamman, J.H., 2008. Gel composition and Application of *Aloe vera* leaf. Molecules 13, 1599–1616. https://doi.org/10.3390/molecules13081599.

Iglesias, I., Sánchez-Viscaíno, J.M., Muñoz, M.J., Martínez, M., de la Torre, A., 2011. Spatio-temporal model of avian influenza spread risk. Procedia Environ. Sci. 7, 104–109 doi: 10.16/j.proenv.201107.019.

Kojo, E., Qian, H., 2004. *Aloe vera*: a valuable ingredient for the food, pharmaceutical and cosmetic industries-a review. Crit. Rev. Food Sci. Nutr. 44, 91–96. https://doi.org/10.1080/10408690490424694.

Lee, T.S., Das, A., Knosla, C., 2007. Structure-activity relationships of semisynthetic mumbaistatin analogs. Bioorg. Med. Chem. 15, 5207–5218. https://doi.org/1016/j.bmc.2007.05.019.

Li, S.W., Yang, T.C., Lai, C.C., Huang, S.H., Liao, J.M., Wan, L., Lin, Y.J., Lin, C.W., 2014. Antiviral activity of aloe-emodin against influenza A virus via galectin-3-up-regulation. Eur. J. Pharmacol. 738, 125–132. https://doi.org/1016/j.ejphar.2014.05.028.

Li, T.C.M., Chan, M.C.W., Lee, N., 2015. Clinical implications of antiviral resistance in influenza. Viruses 7, 4929–4944. https://doi.org/10.3390/v7092850.

McKimm-Breschkin, J., 2013. Influenza neuraminidase inhibitors: antiviral action and mechanisms of resistance. Influenza Other Respir. Viruses 7, 25–36. https://doi.org/10.1111/irv.12047.

Naesens, L., Stevaert, A., Vanderlinden, E., 2016. Antiviral therapies on the horizon for influenza. Curr. Opin. Pharmacol. 30, 106–115. https://doi.org/1016/j.coph.2016.08.003.

Nishikawa, T., Shimizu, K., Tanaka, T., Kuroda, K., Takayama, T., Yamamoto, T., Hanada, N., Hamada, Y., 2012. Bacterial neuraminidase rescues influenza virus replication from inhibition by a neuraminidase inhibitor. PLoS One 7, e45371. https://doi.org/101371/journal.pone.0045371.

Park, J.Y., Kim, J.H., Kim, Y.M., Jeong, H.J., Kim, D.W., Park, K.H., Kwon, H.J., Park, S.J., Lee, W.S., Ryu, Y.B., 2012. Tanshinones as selective and slow-binding inhibitors for SARS-CoV cysteine proteases. Bioorg. Med. Chem. 20, 5928–5935. https://doi.org/1016/j.bmc.2012.07.038.

Reynolds, T., 1985. Observations on the phytochemistry of the aloe leaf-exudate compounds. Bot. J. Linn. Soc. 90, 179–199. https://doi.org/10.1111j.1095.8339.1985.tb00378.x.

Reynolds, T., Dweck, A., 1999. *Aloe vera* leaf gel: a review update. J. Ethnopharmacol. 68, 3–37.

Salah, F., Ghoul, Y.H., Mahdhi, A., Majdoub, H., Jarroux, N., Sakli, F., 2017. Effect of the deacetylation degree on the antibacterial and antibiofilm activity of acemannan from Aloe vera. Ind. Crops Prod. 103, 13–18. https://doi.org/1016/j.indocrop.2017.03.031.

SIAP, 2015. Servicio De Información Agroalimentaria Y Pesqueria, México. Consulted on july 2018.. (Accessed 19 July 2018). http://www/Index.jsp.

Sidwell, R.W., Smee, D.F., 2000. *In vitro* and *in vivo* assay systems for study of influenza virus inhibitors. Antiviral Res. 48, 1–16.

Sydiskis, R.J., Owen, D.G., Lohr, J.L., Rosler, K.H.A., Blomster, R.N., 1991. Inactivation of enveloped viruses by anthraquinones extracted from plants. Antimicrob. Agents Chemother. 35, 2463–2466.

Taubenberger, J.M.D., 2008. The pathology of influenza virus infections. Annu. Rev. Pathol. 3, 499–522.

Wang, J., Xiaochu Qin, Z., Ju, Z., He, W., Tan, Y., Zhou, X., Tu, Z., Lu, F., Liu, Y., 2016. Two new anthraquinones with antiviral activities from the barks of *Morinda citrifolia* (Noni). Phytochem. Lett. 15, 13–15. https://doi.org/1016/j.phytol.2015.11.006.

Yagi, A., Makino, K., Nishioka, I., 1974. Studies on the constituents of *Aloe saponaria* Haw, I. The structures of tetrahydroantracene derivatives and related anthraquinones. Chem. Pharm. Bull. 22, 1159–1166. https://doi.org/10.1248/cpb.22.1159.

Yamada, K., Koyama, H., Hagiwara, K., Ueda, A., Sasaki, Y., Kanesashi, S.N., Ueno, R., Nakamura, H.K., Kuwata, K., Shimizu, K., Suzuki, M., Aida, Y., 2012. Identification of a novel compound with antiviral activity against influenza A virus depending on PA subunit of viral RNA polymerase. Microbes Infect. 14, 740–747. https://doi.org/1016/j.micinf.2012.02.012.

Yang, Z., Yang, Y., Wu, F., Feng, X., 2013. Computational investigation of interaction mechanisms between juglone and influenza virus surface glycoproteins. Mol. Simul. 39, 788–795. https://doi.org/10.1080/08927022.2013.769683.

Zhang, J., Liu, T., Tong, X., Li, G., Yan, J., Ye, X., 2012. Identification of novel virus inhibitors by influenza A virus specific reporter cell based screening. Antiviral Res. 93, 48–54. https://doi.org/1016/j.antiviral.2011.10.014.